How to cite: *Angew. Chem. Int. Ed.* **2022,** *61,* e202204565
International Edition: doi.org/10.1002/anie.202204565
German Edition: doi.org/10.1002/ange.202204565

Enzyme Inhibitors

Aryl Fluorosulfate Based Inhibitors That Covalently Target the SIRT5 Lysine Deacylase**

*Julie E. Bolding[+], Pablo Martín-Gago[+], Nima Rajabi, Luke F. Gamon, Tobias N. Hansen, Christian R. O. Bartling, Kristian Strømgaard, Michael J. Davies, and Christian A. Olsen**

Abstract: The sirtuin enzymes are a family of lysine deacylases that regulate gene transcription and metabolism. Sirtuin 5 (SIRT5) hydrolyzes malonyl, succinyl, and glutaryl ε-*N*-carboxyacyllysine posttranslational modifications and has recently emerged as a vulnerability in certain cancers. However, chemical probes to illuminate its potential as a pharmacological target have been lacking. Here we report the harnessing of aryl fluorosulfate-based electrophiles as an avenue to furnish covalent inhibitors that target SIRT5. Alkyne-tagged affinity-labeling agents recognize and capture overexpressed SIRT5 in cultured HEK293T cells and can label SIRT5 in the hearts of mice upon intravenous injection of the compound. This work demonstrates the utility of aryl fluorosulfate electrophiles for targeting of SIRT5 and suggests this as a means for the development of potential covalent drug candidates. It is our hope that these results will serve as inspiration for future studies investigating SIRT5 and general sirtuin biology in the mitochondria.

Introduction

The NAD^+-dependent sirtuin (SIRT) enzymes catalyze the cleavage of ε-*N*-acyllysine posttranslational modifications and therefore play key roles in regulating a range of biological processes, including gene transcription and metabolism.[1] Seven different sirtuin isoforms (SIRT1-7), which vary in cellular localization[2] and display preference for different ε-*N*-acyllysine modifications,[3] have been identified in mammals. Among these, SIRT5 primarily localizes to the mitochondria and removes glutaryl,[4] succinyl[5] and malonyl[5,6] posttranslational modifications from lysine residues of a variety of mitochondrial proteins.[7] For example, SIRT5 has been shown to promote detoxification of reactive oxygen species (ROS)[8] and ammonia,[9] inhibit inflammation,[10] modulate mitophagy during starvation,[11] maintain cardiac oxidative metabolism in response to cardiac stress,[12] and regulate mitochondrial metabolism in brown adipose tissue.[13] SIRT5 has also been shown to regulate tumor growth[14] highlighting the therapeutic potential associated with SIRT5 inhibition.[15]

We recently reported compound **1** (Figure 1) as a potent and selective mechanism-based SIRT5 inhibitor.[16] Compound **1** contains a thiourea functionality that enables formation of a stalled intermediate with ADP-ribose during the NAD^+-mediated hydrolysis mechanism of sirtuins, therefore enhancing its residence time inside the SIRT5 substrate-binding pocket. In addition, **1** contains a terminal carboxylic acid moiety on the modified lysine side chain that mimics the native substrates and forms hydrogen bonds with the Tyr102-Arg105 motif in the active site, which results in selective inhibition of SIRT5 over other sirtuin enzymes (Figure 1A).[16] Due to limitations associated with cell permeability and serum stability, optimization of **1** was necessary to develop SIRT5-targeting inhibitors for applications in living cells. Modifying the carboxylate to give an ethyl ester prodrug[17] or a masked tetrazole isostere[18] provided compounds against SIRT5-dependent acute myeloid leukemia cell lines,[17,18] but the thiourea functionality[19] and hydrophobicity would still cause concern with respect to in vivo applications. Furthermore, the development of covalent inhibitors has proven useful to identify and scrutinize protein function in chemical biology and drug discovery efforts[20] and has even led to the design of targeted covalent inhibitors currently used in the clinic.[21] We therefore envisioned that pursuing a covalently targeted inhibitor strategy for SIRT5 could provide useful chemotypes for its further investigation. To design covalent inhibitors of SIRT5, we hypothesized that the environment around the Tyr102-Arg105 motif could be targeted by identifying a matching electrophilic functional group to be combined with the scaffold of **1**. By applying this strategy,

[*] J. E. Bolding,[+] P. Martín-Gago,[+] N. Rajabi, T. N. Hansen, C. R. O. Bartling, K. Strømgaard, C. A. Olsen
Center for Biopharmaceuticals & Department of Drug Design and Pharmacology, Faculty of Health and Medical Sciences, University of Copenhagen
Universitetsparken 2, DK-2100 Copenhagen (Denmark)
E-mail: cao@sund.ku.dk
L. F. Gamon, M. J. Davies
Department of Biomedical Sciences, Faculty of Health and Medical Sciences, University of Copenhagen
Blegdamsvej 3, DK-2200 Copenhagen (Denmark)
[+] These authors contributed equally to this work.

[**] A previous version of this manuscript has been deposited on a preprint server (https://doi.org/10.26434/chemrxiv-2022-zds91).

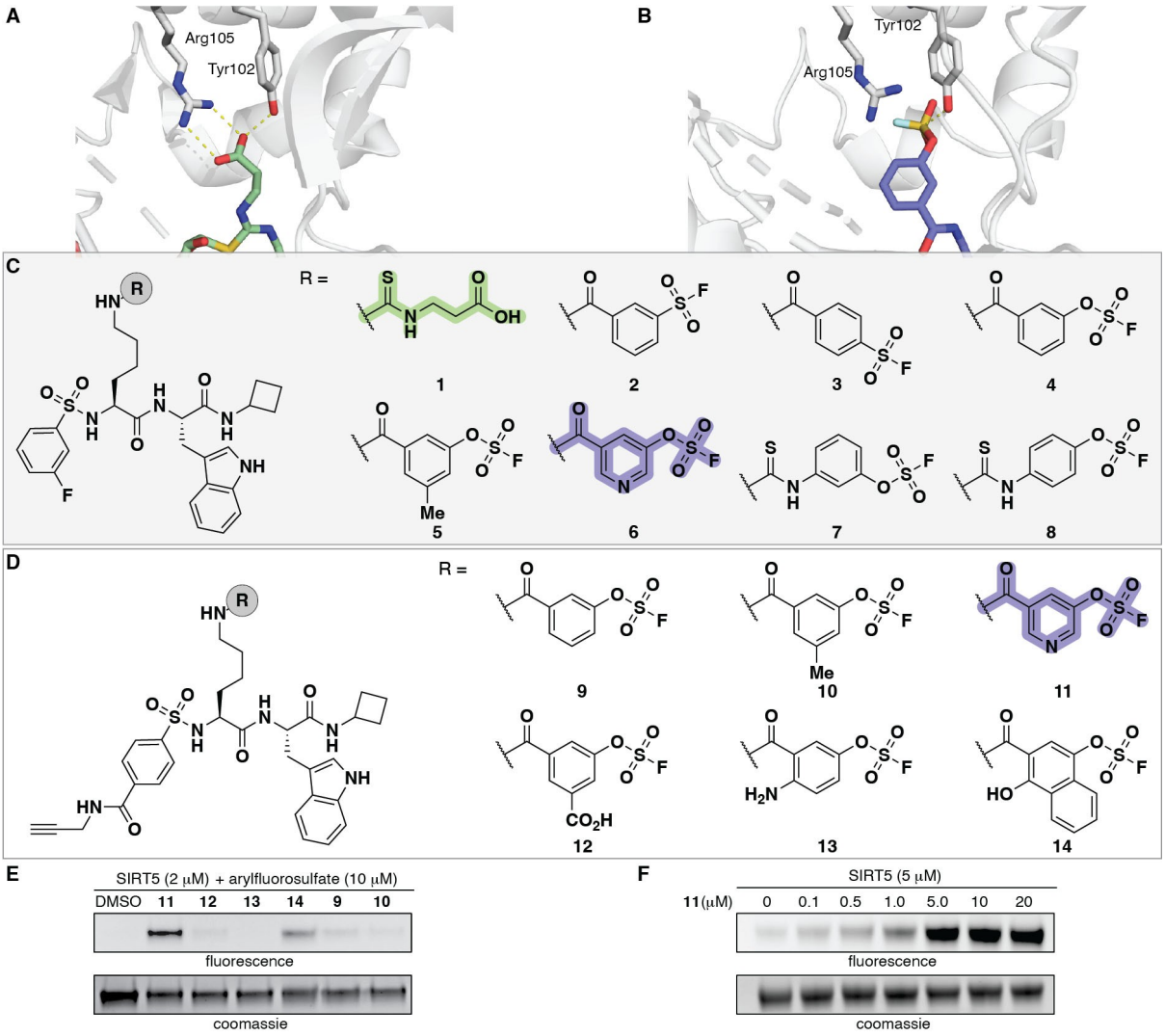

Figure 1. First generation SIRT5-targeting, aryl fluorosulfate-based inhibitors. A) Structure of an analogue of **1** bound to SIRT5 (PDB 6EQS). B) Predicted binding mode of **4** (Schrödinger, Maestro suite), displaying close proximity of the electrophilic sulfur(VI) atom to the Tyr102 side chain. C) Chemical structures of the reversible SIRT5 inhibitor **1** and analogues containing various electrophilic warheads (**2**–**8**). D) Chemical structures containing an alkyne for click chemistry, combined with various electrophilic warheads (**9**–**14**).

we achieved covalent labeling of the SIRT5 enzyme in living cells, which has only been accomplished previously with photo cross-linking chemotypes.[22] Here, the selective targeting of the SIRT5 isoform was achieved with aryl fluorosulfate-based compounds,[23] providing a proof-of-concept for sulfur(VI)-fluoride exchange (SuFEx) chemistry as an enabling technology to target sirtuins.

Results and Discussion

Because of the environment in the active site of SIRT5, we decided to explore SuFEx chemistry[24] for introduction of a latent electrophile into our inhibitors (Figure 1B). Initially, **1** was modified with sulfonyl fluoride-based warheads to afford compounds **2** and **3** (Figure 1C and Supporting Figure S1). However, a considerable degree of double adduct formation was observed (Supporting Figure S3) and we instead turned our attention to fluorosulfates, which are significantly more stable electrophilic sulfur(VI)-fluoride functional groups than sulfonyl fluorides. A requirement for the targeted binding sites of fluorosulfates, is an "appropriate" protein environment for the SuFEx reaction to occur (e.g., basic residues that lower the pK_a of the targeted residue and/or assist in the departure of the fluoride ion).[25] Thus, aryl fluorosulfates display low hydrolytic susceptibility and minimal off-target reactivity in a proteome context[23] and may therefore be promising for targeting pK_a perturbed Tyr, Lys, or Ser residues.[24c] Because the *meta*-substituted compound **2** reacted more readily with SIRT5, we incorporated a selection of *meta*-substituted aryl fluorosulfates onto the scaffold to yield compounds **4**–**6** (Figure 1C and Supporting Figure S1) and MALDI-TOF MS revealed the formation of a covalent conjugate upon incubation of

recombinant SIRT5 with **6** (Supporting Figure S3). In addition, two different aryl fluorosulfates were attached to the parent scaffold via a thiourea functionality (**7** and **8**; Figure 1C and Supporting Figure S1). However, the degree of conjugate formation was not significantly enhanced compared to the amide analogs and the thiourea functionality was abandoned. (Supporting Figure S3).

Next, we synthesized alkyne-containing analogues that would allow us to expand the versatility of these covalent inhibitors for SIRT5 by attachment of either fluorophore- or biotin-functionalized azides using copper(I)-catalyzed Huisgen 3+2 azide-alkyne cycloaddition (CuAAC) "click" chemistry[26] (**9**–**14**, Figure 1D and Supporting Figure S2). For the evaluation of their ability to form covalent adducts with SIRT5, we relied on in-gel fluorescence measurements, taking advantage of the alkyne handle (Supporting Figures S3 and S4). Based on these assays, we decided to continue with the pyridyl fluorosulfates (**6** and **11**). For **11** we could demonstrate dose-dependent labeling down to sub-micromolar compound concentrations, which could be outcompeted by the potent reversible inhibitor **1**, as well as highly selective labeling of SIRT5 over the other recombinant sirtuins (Supporting Figure S3).

To improve aqueous solubility for further applications, we designed a second generation of inhibitors based on insight from our previous structure-activity relationship (SAR) study and X-ray co-crystal structures.[16] These indicated a significant degree of flexibility in the choice of side chain at the $i+1$ position and we therefore substituted the lipophilic Trp residue for an Arg residue at this position to give reversible inhibitor **15** and aryl fluorosulfate-containing compounds **16** and **17**, respectively (Figure 2A and Supporting Figure S5 and S6). In addition, we synthesized compounds **18** and its alkyne-containing analogue **19**, containing the documented mitochondria-targeting triphenylphosphonium motif (Figure 2A and Supporting Figure S7).[27]

The second-generation series was first tested for inhibition of recombinant SIRT5 activity, using our functional fluorogenic assay. For these assays as well as the further evaluations, we expressed a SIRT5 construct that allowed removal of the fused His-tag to better mimic the native state

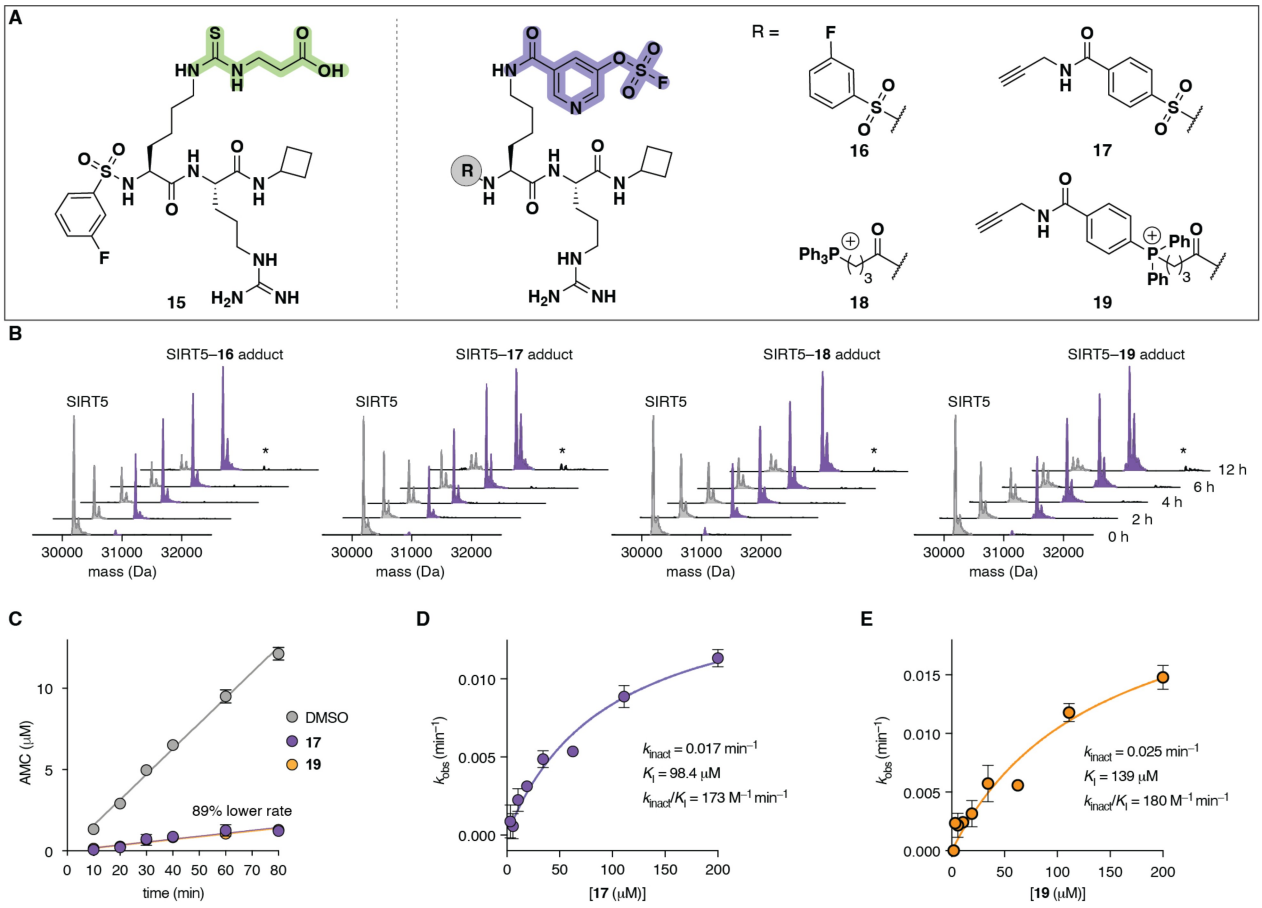

Figure 2. Second generation SIRT5-targeting, aryl fluorosulfate-containing inhibitors. A) Structures of compounds **15**–**19**. B) LC-MS analysis of the time-dependent formation of covalent conjugates between non-tagged recombinant SIRT5 (10 μM) and compounds **16**–**19** (100 μM) in the presence of NAD^+ (200 μM). *Corresponds to a byproduct where SIRT5 has been modified twice by adduct formation. C) Jump dilution assay performed for **17** and **19** after 16 h pre-incubation. D), E) Determination of k_{obs} from time-dependent dose-response experiments and subsequent data fitting to $k_{obs} = (k_{inact} \times [I])/(K_I + [I])$, to derive k_{ianct} and K_I values for **17** and **19**, respectively. For kinetic model, additional equations and plots of the time-dependent inhibition data, see Supporting Figure S10).

of the protein. The reversible inhibitor analogue (**15**) exhibited equipotent activity compared to parent compound **1** and all aryl fluorosulfate-containing compounds (**16**–**19**) exhibited time-dependent inhibition of SIRT5 (Supporting Figure S8).

In agreement with these findings, incubation of recombinant SIRT5 with the four covalently labeling compounds (**16**–**19**), followed by liquid chromatography (LC)-MS analysis, also showed time-dependent formation of enzyme-compound conjugates (Figure 2B and Supporting Figure S9). Moreover, the LC-MS based assays were performed for **16** and **17** both with and without the addition of the NAD^+ co-substrate. A comparison of the degree of covalent binding, showed that the presence of NAD^+ resulted in faster adduct formation, suggesting that the covalent inhibitors act via a mechanism involving the active site of SIRT5.

We then performed a more thorough kinetic evaluation of the inhibitory potencies of our compounds, given that IC_{50} values of covalent inhibitors are inherently time-dependent as also demonstrated here. First, we performed a jump dilution assay with pre-incubation of enzyme and inhibitor **17** or **19** for 16 h and measurement of conversion of substrate at different time points after 100-fold dilution and addition of the substrate. Compared to the DMSO control, the rate of substrate conversion for both compounds were very close to the expected 10 % for an irreversible covalent inhibitor (Figure 2C). Thus, a meaningful measure of the compound potency was warranted and we decided to perform a more substantial series of preincubation experiments to be able to derive the kinetic parameters, k_{inact} and K_I (Figure 2D, E). For irreversible covalent inhibitors, the k_{inact} is the maximal theoretical rate of inactivation of the enzyme, while the K_I is the concentration of inhibitor that provides half-maximal rate of enzyme inactivation [$K_I = (k_{-1} + k_{inact})/k_1$] (see Supporting Figure S10). Thus, $k_{inact} \times K_I^{-1}$ is a measure of the efficiency of the overall conversion of active enzyme to covalently inactivated enzyme. The derived K_I values for our two compounds were in the micromolar range (98–139 μM) and the k_{inact} values were not particularly fast (0.017–0.025 min^{-1}). These values compare well with previously reported kinetic parameters for an aryl fluorosulfate-containing inhibitor, discovered through rounds of phage-display.[28] However, another example of steady-state kinetic parameters for an aryl fluorosulfate-containing probe, reported ≈20-fold higher potency for their target than observed for our compounds.[23] These data show that aryl fluorosulfates react relatively slowly with lower k_{inact} values than for example reported recently for a sulfonyl-fluoride-containing covalent inhibitor,[29] underlining the latent electrophilic nature of the aryl fluorosulfate group.

To address the selectivity of our inhibitors, two alkyne-containing analogues (**17** and **19**) were then incubated with each of the human sirtuin isoforms (Figure 3A and Supporting Figure S11). In-gel fluorescence imaging demonstrated that only incubation with SIRT5 produced covalent adducts with the electrophilic warhead of **17** and **19** to a substantial extent (Figure 3A and Supporting Figure S11). To further substantiate the hypothesis that the compounds bind to the predicted pocket in SIRT5, we first evaluated the importance of a correctly folded protein on conjugate formation, because such a requirement would strongly argue against non-specific binding. We investigated the labeling efficiency of **17** and **19**—as determined by in-gel fluorescence—in standard buffer by pre-boiling the enzyme and under denaturing conditions by addition of sodium dodecyl sulfate (SDS) (Figure 3B and Supporting Figure S12). These experiments showed almost complete disappearance of the bands corresponding to covalent binding when the structural integrity of the enzyme was compromised (Figure 3B and Supporting Figure S12). We interpret these data as indicating that a well-defined binding pocket is necessary to facilitate SuFEx conjugation with our inhibitors (Figure 3B). Furthermore, the reversible inhibitor **1** and a standard fluorogenic SIRT5 substrate (Ac-LGKglut-AMC),[4a] both exhibited dose-dependent competition of the SIRT5-**17** and SIRT5-**19** adduct formation (Figure 3C, D and Supporting Figure S13), providing additional evidence that **17** and **19** covalently label SIRT5 in the substrate-binding pocket.

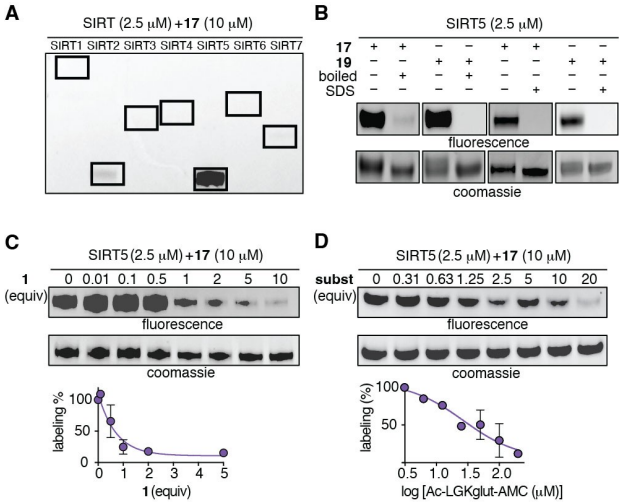

Figure 3. Selectivity for SIRT5 and targeting of its substrate binding pocket. A) Covalent labeling of SIRT1-7 by **17**. Recombinant enzymes (2.5 μM) were incubated with **17** and NAD^+ (200 μM) (all enzymes except SIRT4 were applied in functional assays and shown to be active deacylases; see Supporting Figure S11 for full gel images, repetitions, and similar evaluation of **19**). B) Labeling of non-tagged recombinant SIRT5 by **17** and **19**, with or without pre-boiling or SDS treatment. For full gel images and repetitions see Supporting Figure S12. C) Concentration-dependent competition of the covalent labeling of non-tagged recombinant SIRT5 by **17**, using the reversible inhibitor **1** as competitor. D) Concentration-dependent competition of the covalent labeling of non-tagged recombinant SIRT5 by **17**, using the fluorogenic substrate Ac-LGKglut-AMC as competitor. For compound **19**, full gel images, and repetitions related to (C) and (D), see Supporting Figure S13.

Next, we expressed constructs in which Tyr102 or Arg105 were mutated to phenylalanine (Y102F) and alanine (R105A),[16] respectively, as well as mutants involving the close-by Tyr104 (for activity of the mutants, see Supporting Figure S14). The time-dependent covalent adduct formation between each mutant and the second-generation compounds **16**–**19** was analyzed by LC-MS, which showed substantial

labeling of the SIRT5(Y102F) construct but not SIRT5-(R105A) by all compounds (Figure 4A and Supporting Figure S9). The lack of labeling of the R105A mutant is in agreement with the hypothesis that a basic environment is necessary for SuFEx conjugation between phenolic functional groups and aryl fluorosulfates.[23] However, the SIRT5 mutants that lacked Tyr102 and/or Tyr 104 were still efficiently labeled (Supporting Figure S9c), indicating that there is a conjugation site for our compounds other than Tyr102 and Tyr104. We then performed competition experiments showing that adduct formation between compound **17** or **19** and the three mutants that were susceptible to covalent binding could be inhibited by **1** (Figure 4B and Supporting Figure S15), which provides a further indication that the aryl fluorosulfate-containing compounds **17** and **19** also bind in the active site of the SIRT5 mutants. Thus, the data led us to conclude that activation of the SuFEx reaction by the basic Arg105 residue in the active site is necessary

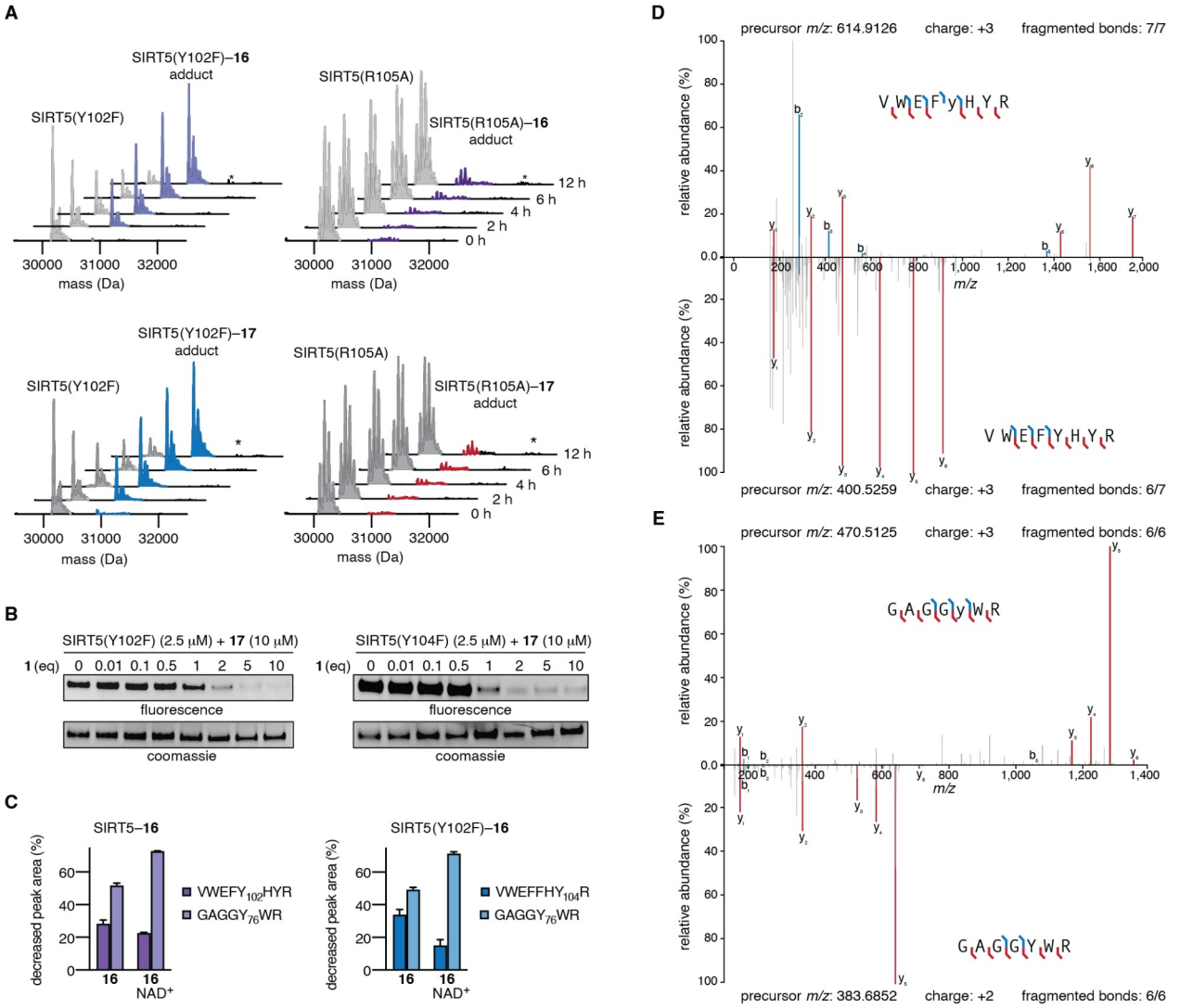

Figure 4. Labeling of SIRT5 wild-type and active site mutants. A) LC-MS analysis of the time-dependent formation of covalent conjugates between recombinant SIRT5(Y102F) and SIRT5(R105A) mutants (10 μM) with compound **17** or **19** (100 μM) in the presence of NAD^+ (additional data, including that for compounds **16**, **18**, and **19** and data for the mutants SIRT5(Y104F) and SIRT5(Y102F/Y104F) are available in the Supporting Information and Supporting Figure S9). *Corresponds to a biproduct where SIRT5 has been modified twice by adduct formation. B) Competition of covalent binding of compound **17** to the mutant enzymes by inhibitor **1**, visualized by in-gel fluorescence. For full gel images and repetitions, see Supporting Figure S15. C) LC-MS/MS analysis of tryptic digests of SIRT5 or SIRT5(Y102F) after incubation with compound **16**. Loss of peptides, $VWEFY_{102}HYR$, $VWEFFHY_{104}R$, and $GAGGY_{76}WR$, due to modification by the covalent inhibitor in the presence or absence of NAD^+. Bars represent the fold change (%) normalized to unmodified samples. D) Representative MS/MS spectrum of the unmodified $VWEFY_{102}HYR$ peptide and mirror of the modified $VWEFY_{102}$[+643.16 Da]HYR peptide after tryptic digestion of recombinant SIRT5. Modification was clearly identified as occurring at Tyr102. The presented *m/z* values are deconvoluted to a +1 charge state for ease of comparison (y5, y6, and y7 were observed as doubly-charged fragments in the raw MS/MS spectrum, see Supporting Information). E) Representative MS/MS spectrum of the unmodified $GAGGY_{76}WR$ peptide and mirror of the modified $GAGGY_{102}$[+643.16 Da]WR peptide after tryptic digestion of recombinant SIRT5. Modification was clearly identified at Tyr76. For data regarding modification of SIRT5(Y102F) on $VWEFFHY_{104}RR$, additional data, and repetitions, see Supporting Figures S16–S18.

and we hypothesized that while activated in the substrate binding pocket, the fluorosulfate can label more than one amino acid in SIRT5.

To further investigate the site of covalent cojugation, we obtained peptide mass fingerprinting data by LC-MS/MS analysis upon tryptic digestion of enzyme-compound conjugates from incubation of wild-type SIRT5 and SIRT5-(Y102F) with **16** (Supporting Figures S16–18). These experiments showed that the compounds can indeed form a covalent conjugate with Tyr102 but could also target residue Tyr76, which resides in a flexible loop of SIRT5 according to X-ray crystal structures[4b,5,16] (Figure 4C–E and Supporting Figures S16–18).

In the absence of Tyr102 in the SIRT5(Y102F) mutant, compound **16** formed covalent conjugates with both Tyr104 and Tyr76 (Figure 4C and Supporting Figures S16–18). Interestingly, it appeared from the measured as loss of peptide (Figure 4C), that the presence of NAD^+ caused an increase in the ratio of the Tyr76 conjugate, while it caused a decrease in the labeling of the $VWEFY_{102}HYR$/$VWEFFHY_{104}R$/$VWEFFHY_{104}RR$ peptides, indicating a conformational change caused by binding of NAD^+ to favor conjugation to the more distant Tyr76.

Because the compounds react relatively slowly as shown by the kinetics experiments, a high degree of stability is necessary for fluorosulfates to be applicable in cell-based assays. We therefore tested the chemical stability of compounds **16**–**19** in assay buffer as well as in assay buffer with reduced glutathione added. All compounds exhibited long half-lives; albeit, with a decrease when glutathione was included in the buffer (Figure 5A, B), which is in agreement with previous studies on ^{18}F positron emission tomography (PET) tracers.[30] Compounds **18** and **19** were also slightly less stable than their counterparts lacking the triphenylphosphonium motif (Supporting Figure S18). Next, we evaluated the relative overall ability of our fluorosulfate compounds to penetrate the cellular plasma membrane, compared to previously developed inhibitors **1** and **1-Et**, by applying the chloroalkane cell-penetration assay (CAPA) procedure.[31] We attached the chloroalkane (CA) at the N-terminal to give CA-tagged versions of a Trp- and an Arg-containing fluorosulfate (**20** and **21**; Figure 5C and Supporting Figure S19). The relative ability of compounds **20** and **21** to enter cells in culture, compared to the positive control compound **CA-Trp-OH** (tryptophan α-*N*-acylated with the same chloroalkane) and previously prepared CA-containing versions of **1** and **1-Et**,[18] were analyzed in a HaloTag-expressing HeLa cell line (Figure 5D). These assays revealed similar degree of cell penetration for our fluorosulfate compounds as recorded for the positive control (**CA-Trp-OH**) and CA-tagged prodrug "**CA-1-Et**", while the free carboxylate analogue "**CA-1**" exhibited substantially lower ability to penetrate the cells.

These results encouraged us to investigate the inhibitors in cells and we first attempted a cellular thermal shift assay using western blotting to evaluate target engagement based on the resulting melting curves for SIRT5. Unfortunately, we only observed a small destabilizing effect (Supporting Figure S20) and instead turned to labeling of the enzyme in

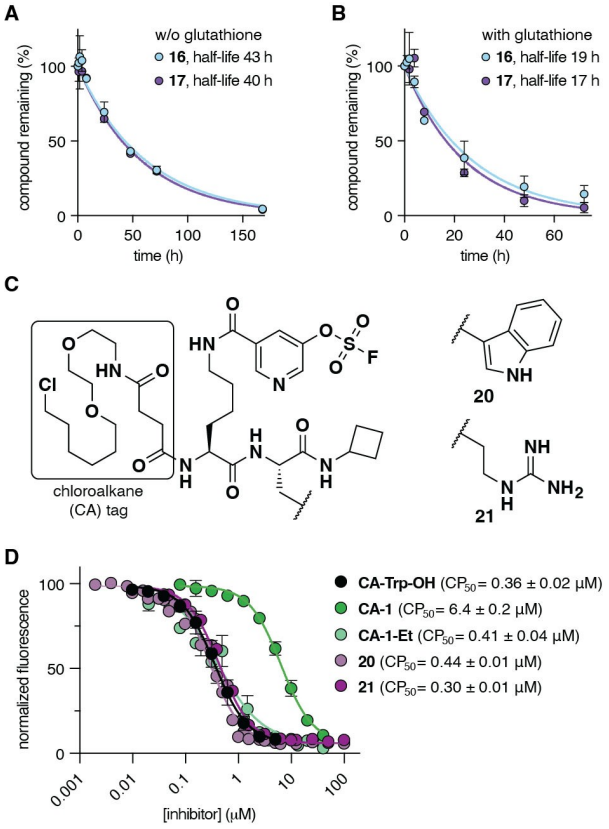

Figure 5. Chemical stability of compounds 16 and 17. A) Stability in HDAC assay buffer at 37 °C measured by HPLC. B) Stability in HDAC assay buffer, containing reduced glutathione (GSH; 2 mM) at 37 °C. Data are shown as mean values relative to the arbitrary fluoresence units at $t = 0$ h ± SD ($n = 2$). For additional data with compounds **18** and **19**, see Supporting Figure S18). C) Structures of synthesized chloroalkane probes. D) CAPA results for compounds **20** and **21** as well as the α-*N*-"chloroalkane"-containing tryptophan (**CA-Trp-OH**), compound **1** (**CA-1**),[18] and compound **1-Et** (**CA-1-Et**)[18] after 4 hours of treatment with inhibitor ($n \geq 3$). See the Supporting Information Figure S19 for structures and synthesis of control CAPA compounds.

HEK293T cells. Lysates from wt HEK293T cells and HEK293T cells that overexpress SIRT5-FLAG were harvested and both were shown to exhibit desuccinylase and deglutarylase activity that could be inhibited by preincubation with compound **16** (Supporting Figure S21). However, incubation with alkyne-containing compounds **17** and **19** at varying concentrations (1–20 μM) only furnished reproducible labeling and pull-down when SIRT5 was overexpressed. Pull-down of SIRT5 was achieved by subjecting the lysate to click chemistry with a biotin-azide reagent and incubating the resulting conjugates with streptavidin-containing magnetic beads for enrichment. Release of the enriched proteins after extensive washing of the beads, followed by SDS-PAGE, and immunoblotting with anti-SIRT5 antibody showed that the compounds **17** and **19** efficiently enabled pull-down of SIRT5 from the lysate in a dose-dependent manner in cells overexpressing SIRT5 (Figure 6A and Supporting Figure S22). Further, these pull-downs could be outcompeted by the addition of reversible

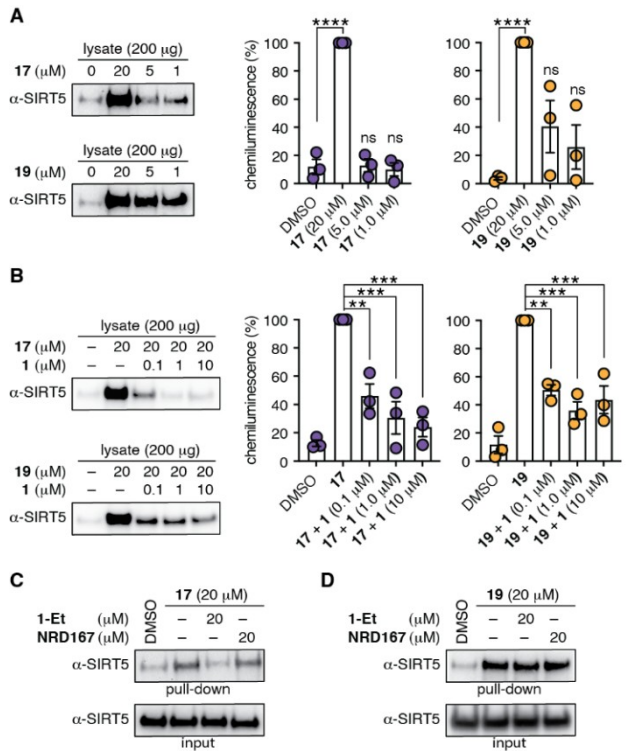

Figure 6. Targeting SIRT5 in cell lysates and living cells. A) Dose-dependent pull-down of overexpressed SIRT5-FLAG in HEK293T cell lysate by compounds **17** and **19**. Bar graphs represent % chemiluminescence signal, normalized to the band for 20 μM treatment ($n=3$; for full gel images, replicates and conditions, see Supporting Figure S22). B) Competition of the covalent conjugate formation with overexpressed SIRT5-FLAG in HEK293T cell lysate (with **17** or **19** at 20 μM) by cotreatment with **1**. Bar graphs represent % chemiluminescence signal, normalized to the band for 20 μM treatment with **17** or **19** ($n=3$; for full gel images, replicates, and conditions, see Supporting Figure S23). C) Labeling and competition of the labeling of overexpressed SIRT5-FLAG in cultured HEK293T cells with **17** (20 μM, 5 h treatment) by cotreatment with prodrugs **1-Et** or **NRD167**. D) Labeling and competition of the labeling, of overexpressed SIRT5-FLAG in cultured HEK293T cells with **19** (20 μM, 5 h treatment) by cotreatment with prodrugs **1-Et** or **NRD167**. Experiments shown in (C), (D) were repeated twice with similar results; for structures of compounds, full gel images, replicates, and conditions, see Supporting Figure S24. Significance of the levels of pulled-down SIRT5 were calculated using one-way ANOVA and Turkey's multiple comparison tests. Adjusted p values are in comparison to treatment with DMSO (A) or covalent inhibitors **17** or **19** without competitor (B): ns denotes $p>0.05$, $*p<0.05$, $**p<0.01$, $***p<0.001$, $****p<0.0001$.

inhibitor **1**, showing that the compounds label SIRT5 through specific binding in the active site (Figure 6B and Supporting Figure S23).

Cultured HEK293T cells overexpressing SIRT5-FLAG were then incubated with compounds **17** and **19** for 5 h at 20 μM concentration and subsequent pull-down experiments, as described above, showed substantial capture of SIRT5 in viable cells, when compared to control cells treated with the carrier DMSO (Figure 6C,D and Supporting Figure S24). Furthermore, when the cells were co-treated with compound **17** and a cellularly active prodrug of **1** (**NRD167**[16] or **1-Et**[17]), the covalent adduct formation between **17** and SIRT5 was efficiently inhibited by **1-Et** and to a lesser extent by **NRD167** in cultured cells (Figure 6C and Supporting Figure S24).

In contrast, adduct formation with compound **19** proved more difficult to outcompete in living cells (Figure 6D and Supporting Figure S24), which we speculate to be due to more limited mitochondrial targeting of the competitive inhibitors, which do not contain the triphenylphosphonium group. Such differences in localization may open the possibility of reporting on different populations of SIRT5 in the cell, i.e. cytosolic vs mitochondrial. However, additional experiments are required to interrogate this idea further.

Next, we applied a recently developed assay that reports on SIRT5 activity in HeLa cells by application of a substrate that self assembles to form fluorescent fibrils upon SIRT5-mediated desuccinylation in the mitochondria.[32] This showed that compound **16** and **17** also inhibit the activity of SIRT5 in living cells (Supporting Figure S25). The potency of **16** proved insufficient to kill cancer cells in culture as demonstrated for our reversible inhibitors,[18] with only limited effect on cell viability detected at concentrations of the compound of up to 200 μM (Supporting Figure S26).

Finally, we envisioned that the latent electrophilicity and high selectivity for SIRT5 could allow for applicability of our compounds beyond cell-based assays as aryl fluorosulfates have previously been applied as electrophiles in probes with efficacy in both *C. elegans*[33] and mice.[34] Furthermore, we were interested in evaluating whether the stability and bioavailability of the compounds would render them fit for further development into lead compounds suitable for drug discovery efforts. Thus, stability in serum was measured, which revealed substantial improvement compared to the parent compound **1** (Figure 7A). We chose to test our compounds in mice by intravenous (i.v.) injection of a single dose of compound **17** or **19** (12 mg kg^{-1}). This dose was well tolerated (albeit, with a slightly sedative effect) for **17**, but resulted in rapid death with compound **19**, presumeably due to the triphenylphosphonium mitochondria-targeting group. Compound **19** was therefore excluded from further animal studies. Blood samples were drawn from different groups of animals (5 mice per group) at various time points and the amount of remaining compound quantified by HPLC; these experiments showed a rapid decrease in blood concentration, and near complete elimination by the 5 min time points (data not shown).

This was substantially faster than what would be expected on the basis of the half-lives of the compounds in serum. However, in addition to degradation and clearance of the compound, distribution to various tissues and organs could also play a significant role in their elimination from the blood stream. We therefore harvested the hearts from mice upon sacrificing them at 6 or 24 h (Figure 7B). The heart was chosen because SIRT5 is highly expressed in cardiac tissue and has been shown to have a unique role in this organ.[35] The hearts were homogenized and lysed followed by click chemistry with the biotin-azide reagent. Subsequent enrichment using streptavidin beads and western blot analysis showed that SIRT5 could be labeled by **17**

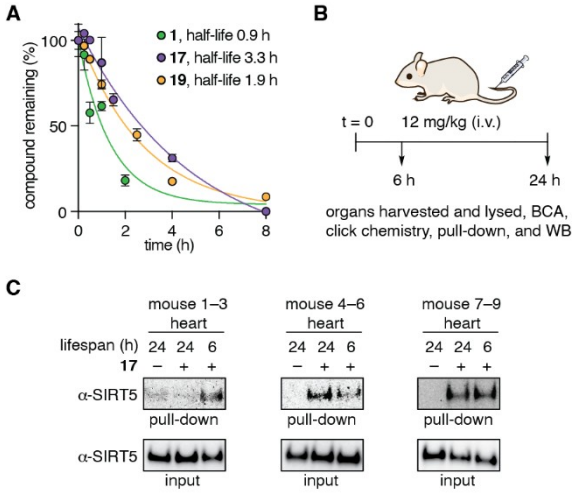

Figure 7. Compound stability and labeling of SIRT5 in vivo. A) Stability of compounds **1**, **17**, and **19** in human serum at 37 °C. Aliquots were collected at different time points, quenched with urea, and partitioned between trichloroacetic acid-acetone (1 : 9) by centrifugation (14000 g). The amount of compound left in the supernatant was analyzed by HPLC. B) Pull-down of labeled SIRT5 in hearts from mice injected with a single dose of **17** (i.v., 12 mg kg^{-1}) and sacrificed after 6 or 24 h. The lysates from hearts were subjected to click chemistry with biotin-N_3, followed by enrichment using streptavidin beads, SDS-PAGE, and western blot analysis. C) Examples of western blots of SIRT5 pull-downs from harvested organs. For additional data and conditions, see Supporting Figure S27.

and enriched as compared to vehicle treated control animals (Figure 7C). Together, these results suggest that compound **17** attains covalent target engagement of SIRT5 in mouse organs, despite rapid clearance from the blood stream.

Conclusion

Through several lines of evidence, we substantiate the claim that our novel aryl fluorosulfates bind covalently to SIRT5 via the enzyme's active site to achieve selectivity over other sirtuin isoforms. Thus, the adduct formation was eliminated by disrupting the structural integrity of the protein using either heating or addition of detergent (SDS), indicating that an intact binding site is important for formation of the covalent conjugate. Furthermore, the adduct formation was outcompeted with either a SIRT5 substrate or the parent reversible inhibitor (**1**).[16] Binding data recorded with various mutants suggest that the Arg105 residue in the substrate-binding pocket plays an essential role in conjugate formation. Presumably, its guanidinium group assists the electrophilic warhead in undergoing the fluoride substitution reaction required for covalent adduct formation. MS data showed that the covalent bond could be formed with two different Tyr residues, the expected Tyr102 as well as Tyr76. The Tyr76 residue is positioned in a flexible loop according to X-ray crystal structures of SIRT5 (e.g., PDB: 4F4U, 3RIG, 6ACP, and 2B4Y; Supporting Figure S28) and may therefore also engage in the SuFEx reaction with our compounds while they are present in the active site.

Both time-dependent binding studies using LC-MS and determination of steady-state enzyme kinetic inhibition parameters showed that the compounds react with the enzyme over a period of hours, which is to be expected for a latent aryl fluorosulfate electrophile. However, this also places high demands on the compound stability and it was therefore gratifying to find that the half-lives of **16** and **17** in buffer were >17 h even when challenged with glutathione. Together, these results provide a compelling proof of concept for the use of SuFEx chemistry to covalently target SIRT5, while it is also evident that affinity could be improved through follow-up SAR to design compounds with more accurate positioning of the warhead towards the Tyr102 residue in the active site.

Nevertheless, the compounds were shown to exhibit function in viable cultured cells. The ability to capture SIRT5 by covalent adduct formation was demonstrated for the alkyne-containing compounds **17** and **19** in a dose-dependent manner, using intact HEK293T cells overexpressing SIRT5-FLAG. Further, the effect of compound **17** could be outcompeted by co-treatment with reversible SIRT5 inhibitor **1-Et**. Finally, a small preliminary mouse study with alkyne-containing compound **17** showed covalent capturing of SIRT5 in mouse heart tissue by pull-down, enrichment, and western blotting.

We envision that the ability of covalent chemotypes to report on the efficiency of potential new reversible ligands for SIRT5 in cells could be harnessed in future studies of this target. In particular, a combination with proteome-wide mass spectrometry could provide detailed insight into the mechanism and effects of new ligands. It is our hope that the conceptual advance of targeting SIRT5 covalently, provided herein, will serve as a foundation for optimization of chemotypes with potential as probes and/or drug lead compounds.

Supporting Information

Supporting figures, biochemical methods, chemistry and compound characterization, supporting references, LC-MS binding assay data, as well as copies ^{1}H, ^{13}C, and ^{19}F NMR spectra (PDF).

Acknowledgements

We thank M. Bæk and A. L. Nielsen for assistance with pull-down, overexpression, and donation of reagents. We thank S. A. Pless for donation of HEK293T cells as well as insightful comments on the manuscript and J. Kritzer for providing the HaloTag-expressing HeLa cell line. We thank H. S. Larsen and M. Caldara for animal facility assistance and Samuel A. J. Trammell for insightful information on peptide mass fingerprinting. The SIRT5-Flag vector was a gift from E. Verdin (Addgene plasmid #13816). We gratefully acknowledge financial support from the Carlsberg

Foundation (2013-01-033 and CF15-0115, C.A.O.), the Novo Nordisk Foundation (NNF17OC0029464, C.A.O.; NNF13OC0004294, M.J.D.), the Lundbeck Foundation (R289-2018-2074, C.A.O.; R322-2019-2337, L.F.G.), and the Independent Research Fund Denmark-Medical Sciences (0134-00435B; C.A.O.). This project has received funding from the European Research Council (ERC) under the European Union's Horizon 2020 Research and Innovation Programme (grant agreement number: CoG-725172 "*SIR-FUNCT*"; C.A.O.).

Conflict of Interest

The authors declare no conflict of interest.

Data Availability Statement

Raw and processed mass spectrometry data has been deposited in the Mass Spectrometry Interactive Virtual Environment (MassIVE) database. Data can be accessed at ftp://massive.ucsd.edu/MSV000087758 with doi:10.25345/C5F53D. Deposited data includes standardized ".mzML" and raw Bruker ".d" files as well as processed XCMS Online, MaxQuant, and Skyline output files.

Keywords: Covalent Inhibition · Enzyme Inhibitors · SIRT5 · Sirtuins · SuFEx

[1] a) S.-i. Imai, C. M. Armstrong, M. Kaeberlein, L. Guarente, *Nature* **2000**, *403*, 795; b) J. Landry, A. Sutton, S. T. Tafrov, R. C. Heller, J. Stebbins, L. Pillus, R. Sternglanz, *Proc. Natl. Acad. Sci. USA* **2000**, *97*, 5807–5811; c) P. Bheda, H. Jing, C. Wolberger, H. Lin, *Annu. Rev. Biochem.* **2016**, *85*, 405–429.

[2] a) R. A. Frye, *Biochem. Biophys. Res. Commun.* **2000**, *273*, 793–798; b) R. Marmorstein, *Structure* **2001**, *9*, 1127–1133; c) E. Michishita, J. Y. Park, J. M. Burneskis, J. C. Barrett, I. Horikawa, *Mol. Biol. Cell* **2005**, *16*, 4623–4635.

[3] a) C. Choudhary, B. T. Weinert, Y. Nishida, E. Verdin, M. Mann, *Nat. Rev. Mol. Cell Biol.* **2014**, *15*, 536–550; b) B. R. Sabari, D. Zhang, C. D. Allis, Y. Zhao, *Nat. Rev. Mol. Cell Biol.* **2017**, *18*, 90–101.

[4] a) M. Tan, C. Peng, K. A. Anderson, P. Chhoy, Z. Xie, L. Dai, J. Park, Y. Chen, H. Huang, Y. Zhang, J. Ro, G. R. Wagner, M. F. Green, A. S. Madsen, J. Schmiesing, B. S. Peterson, G. Xu, O. R. Ilkayeva, M. J. Muehlbauer, T. Braulke, C. Mühlhausen, D. S. Backos, C. A. Olsen, P. J. McGuire, S. D. Pletcher, D. B. Lombard, M. D. Hirschey, Y. Zhao, *Cell Metab.* **2014**, *19*, 605–617; b) C. Roessler, T. Nowak, M. Pannek, M. Gertz, G. T. T. Nguyen, M. Scharfe, I. Born, W. Sippl, C. Steegborn, M. Schutkowski, *Angew. Chem. Int. Ed.* **2014**, *53*, 10728–10732; *Angew. Chem.* **2014**, *126*, 10904–10908.

[5] J. Du, Y. Zhou, X. Su, J. J. Yu, S. Khan, H. Jiang, J. Kim, J. Woo, J. H. Kim, B. H. Choi, B. He, W. Chen, S. Zhang, R. A. Cerione, J. Auwerx, Q. Hao, H. Lin, *Science* **2011**, *334*, 806–809.

[6] C. Peng, Z. Lu, Z. Xie, Z. Cheng, Y. Chen, M. Tan, H. Luo, Y. Zhang, W. He, K. Yang, B. M. M. Zwaans, D. Tishkoff, L. Ho, D. Lombard, T.-C. He, J. Dai, E. Verdin, Y. Ye, Y. Zhao, *Mol. Cell. Proteomics* **2011**, *10*, M111.012658.

[7] a) M. J. Rardin, W. He, Y. Nishida, J. C. Newman, C. Carrico, S. R. Danielson, A. Guo, P. Gut, A. K. Sahu, B. Li, R. Uppala, M. Fitch, T. Riiff, L. Zhu, J. Zhou, D. Mulhern, R. D. Stevens, O. R. Ilkayeva, C. B. Newgard, M. P. Jacobson, M. Hellerstein, E. S. Goetzman, B. W. Gibson, E. Verdin, *Cell Metab.* **2013**, *18*, 920–933; b) B. Chen, W. Zang, J. Wang, Y. Huang, Y. He, L. Yan, J. Liu, W. Zheng, *Chem. Soc. Rev.* **2015**, *44*, 5246–5264; c) Y. Nishida, M. J. Rardin, C. Carrico, W. He, A. K. Sahu, P. Gut, R. Najjar, M. Fitch, M. Hellerstein, B. W. Gibson, E. Verdin, *Mol. Cell* **2015**, *59*, 321–332; d) Y. Du, H. Hu, C. Hua, K. Du, T. Wei, *Biochem. Biophys. Res. Commun.* **2018**, *503*, 763–769.

[8] Z.-F. Lin, H.-B. Xu, J.-Y. Wang, Q. Lin, Z. Ruan, F.-B. Liu, W. Jin, H.-H. Huang, X. Chen, *Biochem. Biophys. Res. Commun.* **2013**, *441*, 191–195.

[9] T. Nakagawa, D. J. Lomb, M. C. Haigis, L. Guarente, *Cell* **2009**, *137*, 560–570.

[10] F. Wang, K. Wang, W. Xu, S. Zhao, D. Ye, Y. Wang, Y. Xu, L. Zhou, Y. Chu, C. Zhang, X. Qin, P. Yang, H. Yu, *Cell Rep.* **2017**, *19*, 2331–2344.

[11] H. Guedouari, T. Daigle, L. Scorrano, E. Hebert-Chatelain, *Biochim. Biophys. Acta Mol. Cell Res.* **2017**, *1864*, 169–176.

[12] K. A. Hershberger, D. M. Abraham, A. S. Martin, L. Mao, J. Liu, H. Gu, J. W. Locasale, M. D. Hirschey, *J. Biol. Chem.* **2017**, *292*, 19767–19781.

[13] G. Wang, J. G. Meyer, W. Cai, S. Softic, M. E. Li, E. Verdin, C. Newgard, B. Schilling, C. R. Kahn, *Mol. Cell* **2019**, *74*, 844–857 e847.

[14] a) W. Lu, Y. Zuo, Y. Feng, M. Zhang, *Tumour Biol.* **2014**, *35*, 10699–10705; b) Y. Xiangyun, N. Xiaomin, G. linping, X. Yunhua, L. Ziming, Y. Yongfeng, C. Zhiwei, L. Shun, *Oncotarget* **2017**, *8*, 6984–6993; c) X. Yang, Z. Wang, X. Li, B. Liu, M. Liu, L. Liu, S. Chen, M. Ren, Y. Wang, M. Yu, B. Wang, J. Zou, W. G. Zhu, Y. Yin, W. Gu, J. Luo, *Cancer Res.* **2018**, *78*, 372–386.

[15] S. Kumar, D. B. Lombard, *Crit. Rev. Biochem. Mol. Biol.* **2018**, *53*, 311–334.

[16] N. Rajabi, M. Auth, K. R. Troelsen, M. Pannek, D. P. Bhatt, M. Fontenas, M. D. Hirschey, C. Steegborn, A. S. Madsen, C. A. Olsen, *Angew. Chem. Int. Ed.* **2017**, *56*, 14836–14841; *Angew. Chem.* **2017**, *129*, 15032–15037.

[17] D. Yan, A. Franzin, A. D. Pomicter, B. J. Halverson, O. Antelope, C. C. Mason, J. M. Ahmann, A. V. Senina, N. A. Vellore, C. L. Jones, M. S. Zabriskie, H. Than, M. J. Xiao, A. van Scoyk, A. B. Patel, P. M. Clair, W. L. Heaton, S. C. Owen, J. L. Andersen, C. M. Egbert, J. A. Reisz, A. D'Alessandro, J. E. Cox, K. C. Gantz, H. M. Redwine, S. M. Iyer, J. S. Khorashad, N. Rajab, C. A. Olsen, T. O'Hare, M. W. Deininger, *Blood Cancer Discovery* **2021**, *2*, 266–287.

[18] N. Rajabi, T. N. Hansen, A. L. Nielsen, H. T. Nguyen, M. Bæk, J. E. Bolding, O. O. Bahlke, S. E. G. Petersen, C. R. O. Bartling, K. Strømgaard, C. A. Olsen, *Angew. Chem. Int. Ed.* **2022**, *61*, e202115805; *Angew. Chem.* **2022**, *134*, e202115805.

[19] N. Rajabi, A. L. Nielsen, C. A. Olsen, *ACS Med. Chem. Lett.* **2020**, *11*, 1886–1892.

[20] T. Zhang, J. M. Hatcher, M. Teng, N. S. Gray, M. Kostic, *Cell Chem. Biol.* **2019**, *26*, 1486–1500.

[21] a) T. A. Baillie, *Angew. Chem. Int. Ed.* **2016**, *55*, 13408–13421; *Angew. Chem.* **2016**, *128*, 13606–13619; b) Z. Zhao, P. E. Bourne, *Drug Discovery Today* **2018**, *23*, 727–735.

[22] a) X. Bao, Y. Wang, X. Li, X. M. Li, Z. Liu, T. Yang, C. F. Wong, J. Zhang, Q. Hao, X. D. Li, *eLife* **2014**, *3*, e02999; b) T. Yang, Z. Liu, X. D. Li, *Chem. Sci.* **2015**, *6*, 1011–1017; c) E. Graham, S. Rymarchyk, M. Wood, Y. Cen, *ACS Chem. Biol.* **2018**, *13*, 782–792; d) M. Bæk, P. Martin-Gago, J. S. Laursen, J. L. H. Madsen, S. Chakladar, C. A. Olsen, *Chem. Eur. J.* **2020**, *26*, 3862–3869.

[23] W. Chen, J. Dong, L. Plate, D. E. Mortenson, G. J. Brighty, S. Li, Y. Liu, A. Galmozzi, P. S. Lee, J. J. Hulce, B. F. Cravatt, E. Saez, E. T. Powers, I. A. Wilson, K. B. Sharpless, J. W. Kelly, *J. Am. Chem. Soc.* **2016**, *138*, 7353–7364.

[24] a) J. Dong, L. Krasnova, M. G. Finn, K. B. Sharpless, *Angew. Chem. Int. Ed.* **2014**, *53*, 9430–9448; *Angew. Chem.* **2014**, *126*, 9584–9603; b) A. S. Barrow, C. J. Smedley, Q. Zheng, S. Li, J. Dong, J. E. Moses, *Chem. Soc. Rev.* **2019**, *48*, 4731–4758; c) P. Martin-Gago, C. A. Olsen, *Angew. Chem. Int. Ed.* **2019**, *58*, 957–966; *Angew. Chem.* **2019**, *131*, 969–978; d) S. Kitamura, Q. Zheng, J. L. Woehl, A. Solania, E. Chen, N. Dillon, M. V. Hull, M. Kotaniguchi, J. R. Cappiello, S. Kitamura, V. Nizet, K. B. Sharpless, D. W. Wolan, *J. Am. Chem. Soc.* **2020**, *142*, 10899–10904.

[25] a) O. O. Fadeyi, L. R. Hoth, C. Choi, X. Feng, A. Gopalsamy, E. C. Hett, R. E. Kyne, R. P. Robinson, L. H. Jones, *ACS Chem. Biol.* **2017**, *12*, 2015–2020; b) D. E. Mortenson, G. J. Brighty, L. Plate, G. Bare, W. Chen, S. Li, H. Wang, B. F. Cravatt, S. Forli, E. T. Powers, K. B. Sharpless, I. A. Wilson, J. W. Kelly, *J. Am. Chem. Soc.* **2018**, *140*, 200–210.

[26] a) V. V. Rostovtsev, L. G. Green, V. V. Fokin, K. B. Sharpless, *Angew. Chem. Int. Ed.* **2002**, *41*, 2596–2599; *Angew. Chem.* **2002**, *114*, 2708–2711; b) C. W. Tornøe, C. Christensen, M. Meldal, *J. Org. Chem.* **2002**, *67*, 3057–3064; c) A. E. Speers, G. C. Adam, B. F. Cravatt, *J. Am. Chem. Soc.* **2003**, *125*, 4686–4687.

[27] J. Zielonka, J. Joseph, A. Sikora, M. Hardy, O. Ouari, J. Vasquez-Vivar, G. Cheng, M. Lopez, B. Kalyanaraman, *Chem. Rev.* **2017**, *117*, 10043–10120.

[28] Y. Tabuchi, T. Watanabe, R. Katsuki, Y. Ito, M. Taki, *Chem. Commun.* **2021**, *57*, 5378–5381.

[29] P. Udompholkul, C. Baggio, L. Gambini, G. Alboreggia, M. Pellecchia, *J. Med. Chem.* **2021**, *64*, 16147–16158.

[30] Q. Zheng, H. Xu, H. Wang, W. H. Du, N. Wang, H. Xiong, Y. Gu, L. Noodleman, K. B. Sharpless, G. Yang, P. Wu, *J. Am. Chem. Soc.* **2021**, *143*, 3753–3763.

[31] a) E. R. Ballister, C. Aonbangkhen, A. M. Mayo, M. A. Lampson, D. M. Chenoweth, *Nat. Commun.* **2014**, *5*, 5475; b) L. Peraro, Z. Zou, K. M. Makwana, A. E. Cummings, H. L. Ball, H. Yu, Y.-S. Lin, B. Levine, J. A. Kritzer, *J. Am. Chem. Soc.* **2017**, *139*, 7792–7802; c) L. Peraro, K. L. Deprey, M. K. Moser, Z. Zou, H. L. Ball, B. Levine, J. A. Kritzer, *J. Am. Chem. Soc.* **2018**, *140*, 11360–11369.

[32] L. Yang, R. Peltier, M. Zhang, D. Song, H. Huang, G. Chen, Y. Chen, F. Zhou, Q. Hao, L. Bian, M. L. He, Z. Wang, Y. Hu, H. Sun, *J. Am. Chem. Soc.* **2020**, *142*, 18150–18159.

[33] A. Baranczak, Y. Liu, S. Connelly, W. G. Du, E. R. Greiner, J. C. Genereux, R. L. Wiseman, Y. S. Eisele, N. C. Bradbury, J. Dong, L. Noodleman, K. B. Sharpless, I. A. Wilson, S. E. Encalada, J. W. Kelly, *J. Am. Chem. Soc.* **2015**, *137*, 7404–7414.

[34] Q. Li, Q. Chen, P. C. Klauser, M. Li, F. Zheng, N. Wang, X. Li, Q. Zhang, X. Fu, Q. Wang, Y. Xu, L. Wang, *Cell* **2020**, *182*, 85–97 e16.

[35] K. A. Hershberger, A. S. Martin, M. D. Hirschey, *Nat. Rev. Nephrol.* **2017**, *13*, 213–225.

Manuscript received: May 20, 2022
Accepted manuscript online: September 21, 2022
Version of record online: October 21, 2022